**2010 SCEC Report**

# Characterization of Earthquake Slip Distribution of the Central San Jacinto Fault

**J.B. Salisbury and T. Rockwell**
**San Diego State University**

**Ken Hudnut**
**US Geological Survey**

## Introduction

The south-central San Jacinto Fault (SJF) from Hemet southeastward to Clark Valley represents the longest and straightest contiguous segment of the SJF zone (Figure 1); it is exceptionally well localized (Rockwell and Ben-Zion, 2007) and is easily identifiable in the geomorphology. The "Anza Seismicity Gap" (Sanders et al., 1981) falls in the middle of this section of the fault with microseismicity to nearly 20 km depth on the edges of the gap (Sanders and Kanamori, 1984). The Hog Lake trench site, located in the Anza Seismic Gap, records the timing of the past 18 surface ruptures in the past 3800 years with an average return period of about 210 years. Work at Hog Lake dates the most recent event (MRE) at ca. 1790, suggesting this was the November 22, 1800 earthquake (Rockwell et al., 2006).

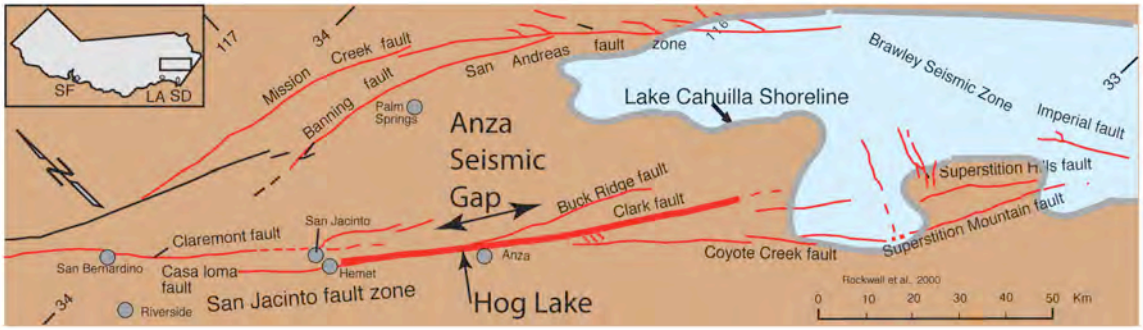


**Figure 1.** *Map of the Southern San Andreas Fault System, highlighting the Clark Fault. Note the overall straight trace of the ~115 km-long Clark-Casa Loma fault, with the "Hemet step-over" to the north and the fault termination to the south.*

In 2006, Middleton evaluated the southern 55 km of the Clark strand of the SJF for offset features using a combination of aerial photography, field techniques, and B4 LiDAR imagery. Displacement estimates show that the MRE produced an average of 2.7 m of dextral slip, with a maximum of 4 m near Anza to less than a meter near the southeast termination of the fault (Figure 2).

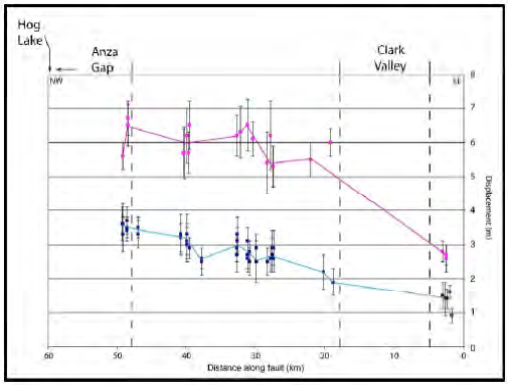


**Figure 2.** *Slip distribution for the past two large surface ruptures on the Clark segment inferred from offset channels and alluvial bars (Middleton, 2006).*

For this continuation project, we completed the work begun by Middleton by mapping the detailed tectonic geomorphology along the remaining 25

km section of the Clark Fault (NW of the Anza Seismicity Gap to Hemet) using aerial photography, B4 LiDAR data, and field techniques. Together, these data provide a robust assessment of the slip distribution for the entire Clark fault in the last few events.

**Methods**

Similar to Middleton, the northwest 25 km of the Clark fault was divided into four major sections (Figure 3). Separated by gorges and, near Anza, the Ramona Indian Reservation, it is in these areas that channel thalwegs, channel margins, and ridge noses were used to measure displacement and compile slip distribution information along the length of the Clark fault.

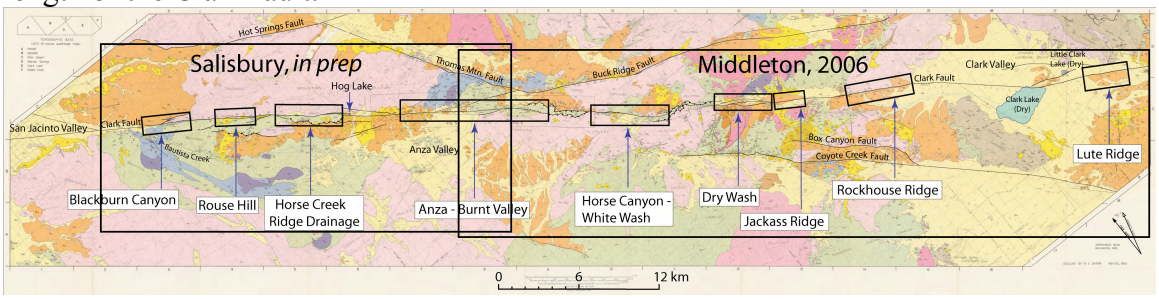


**Figure 3**. *Detailed geologic map of the Clark fault (from Sharp, 1967) showing focus areas of current and past study.*

The elevation of the Clark strand of the SJF varies greatly along strike, from 200-300 m at the southeastern terminus in the Anza Borrego desert to over 1200 m northwest of Anza Valley. In addition to variations in terrain and elevation, increased precipitation and a consequent increase in vegetation density to the northwest of Anza Valley presents a formidable obstacle to both remote and field analysis of the northwestern Clark fault. For this study, significant remote analysis was performed before going into the field.

B4 LiDAR data was acquired as raw, unclassified point clouds via http://www.opentopography.org and gridded for viewing in ESRI's ArcMap. These coarse hillshades were used in conjunction with high-resolution Google Earth Pro images to identify areas with high potential for resolving offset geomorphic features. Small portions of B4 LiDAR data containing prominent fault traces and/or offset features were preferentially selected for vegetation filtering. A multiscale curvature classification algorithm (Evans and Hudak, 2007) was implemented in AML under Arc INFO/Workstation, and 0.25 m resolution digital elevation models (DEM's) were constructed from the classified sections of B4 LiDAR data. These DEM's were used for quantitative analysis of offset features in Applied Imagery's Quick Terrain Modeler (QTM) software and Zielke's 2009 MATLAB graphical user interface "LaDiCaoz."

Finally, the high-resolution DEM's were validated in the field using a Panasonic Toughbook CF-19 Tablet + GPS combination. Offset features were located and placemarked on-site in Google Earth, and offset magnitudes and uncertainties were assessed using standard field techniques.

**Observations/Discussion**

Along the northwestern 25 km of the Clark fault, fifty-five distinct fault offset features were located, and a total of seventy-six individual field-based measurements were made. Of the fifty-five features, thirty-nine were discernible in the filtered B4

LiDAR data. All thirty-nine were analyzed using QTM (over one hundred and twenty individual measurements), and twenty-three of these were analyzed using LaDiCaoz.

In 2006, Middleton made three hundred and forty-eight total measurements from field investigations, aerial photography, and the B4 LiDAR dataset along the southern 55 km of the Clark fault. Together, we present over five hundred and sixty individual measurements made from one hundred and twelve different locations along the 70 km length of the Clark fault from the mouth of Blackburn Canyon southeast to the San Felipe Hills near Borrego Springs. Every feature identified in the LiDAR DEM's has been visited and measured in the field.

We filtered these data using a systematic ranking scheme to present only the most reliable estimates of offset magnitude. The quality of field-based and LiDAR-based measurements was rated on a scale of 1-10 (9-10 = Excellent, 7-8.75 = Good, 5.25-6.75 = Fair, and 0-5 = Poor). Field quality estimates (and measurement uncertainty) were based on feature distinctiveness, the prominence of the fault trace, the average size of alluvial material, the degree to which features were projected into the fault trace, the degree of feature degradation, and the density of surrounding vegetation (which limited visibility considerably in some areas). The qualities of LiDAR-based measurements were assessed in a similar fashion. However, each respective characteristic was wholly based on the quality of 0.25 m contours generated from filtered B4 LiDAR data.

For slip distribution calculations, only offset measurements of confidence 7 or greater (good and excellent) were used. Values were averaged where multiple measurements (field or LiDAR-based) existed for a single feature along strike (i.e. channel thalweg, NW and SE channel margins). Finally, field and LiDAR-based measurements were averaged for a single offset value per geomorphic feature along strike.

**Figure 4.** *Offset channel at km 49.2. The fault could be traced into the channel, based on the geomorphology, and the deflection is spatially associated with the fault. The linearity of the channel away from the fault makes this an excellent candidate for inferring displacement.*

Figure 4 shows and example of an excellent offset in Burnt Valley, where the channel makes an abrupt jog at the fault. For this feature at km 49.2 (measured from the southern end of the study area), Tim Middleton measured 2.4-3.6 m in the field and 3.5-3.6 m using LiDAR. We re-measured this same feature in the field and place a combined LiDAR and field offset estimate of 3.6 -1/ +0.5 m, very similar to the earlier estimate by

Middleton. We also evaluated several other offsets described by Middleton, each falling well within the uncertainty of our new measurements. Based on this, we feel comfortable combining the two sets of data.

We construct the combined slip distribution curves for the Clark fault from southeast of Lute Ridge (km 0) northwest to the northern end of Blackburn Canyon (km 76) by utilizing data with a confidence of seven or greater. In areas where discrete features were displaced by two or more fault strands, offset measurements were summed and resulting magnitudes were regarded as minimums (Figure 5). It should be noted that offsets in very young alluvium are present for an additional ~5 km to the southeast of Middleton's zero point, so the minimum rupture length should be increased by that value.

In the upper diagram (a), we attribute the 3-4 m offsets through the Anza region to the most recent event identified at Hog Lake - tentatively the November 22, 1800 earthquake (Toppozada et al., 1981; Rockwell et al., 2006). Of note is the identification of several smaller offsets in Blackburn canyon that look distinctly fresher (younger) than the 3-4 m offsets near Anza. We tentatively attribute these offsets to the M6.9 (Ellsworth, 2010) earthquake in 1918 for which surface rupture is unreported (Rolfe and Strong, 1918). This is not surprising, as accounts of surface rupture reconnaissance in 1918 clearly state that, for various reasons, there was no trip into Blackburn Canyon. Instead, they took Bautista Road around this area and reported neither a rupture at Hog Lake nor any points farther south. We find many small, fresh offsets ranging from 50 cm to nearly 2 m along a ~15 km section of fault that was previously unmapped for tectonic geomorphology in the field. In the same area, we have more subdued offsets that have measured displacements of 3-4 m, similar to those expected for the ca 1800 earthquake near Anza. In this model, slip in 1800 event was lower in Blackburn Canyon than at Anza, and the section of lower slip filled in with an additional event in 1918. It also suggests that slip in the 1800 event continues farther to the northwest than the mouth of Blackburn Canyon.

In model 2 (b), we attribute all of the smaller offsets (0.5-4 m) in Blackburn Canyon to the ca 1800 event, which suggests that the rupture in this event may have terminated at the mouth of Blackburn Canyon. We do not prefer this interpretation because there appear to be two ages of displacements in this cluster, with the smaller offsets appearing fresher than the larger ones. Nevertheless, the current set of data permit this interpretation.

In both models, the average displacement for the most recent event identified at Hog Lake is on the order of 2.5-2.9 m, and, depending on the preferred model, maximum slip near Anza is estimated to be about 3.9 m. The penultimate event (ca 1550) had slightly smaller displacement values, with a maximum slip value close to 3 m. The third event is similar in size, with cumulative displacement of 9-10 m through Anza for the past three events. These geomorphic observations argue for fairly characteristic slip along the Clark fault for at least the past three events.

North of Blackburn Canyon, the fault enters the broad, alluviated San Jacinto valley floor. In addition to historical sedimentation, the valley floor sediments likely have buried small channel offsets and it is not possible to continue this type of geomorphic analysis. North of Hemet, the Casa Loma fault is geomorphically expressed as the primary surface strand, and is essentially a continuation of the Clark fault. This fault zone extends northwest to Mystic Lake where slip steps to the right (NE) across the

active pull-apart to the Clairemont fault. In model 1 (a), displacement from the ca 1800 earthquake appears to persist as far north as the mouth of Blackburn Canyon, and as there are no structural steps farther north until Mystic Lake, it is plausible that the ca 1800 event ruptured north as far as Mystic Lake, or farther.

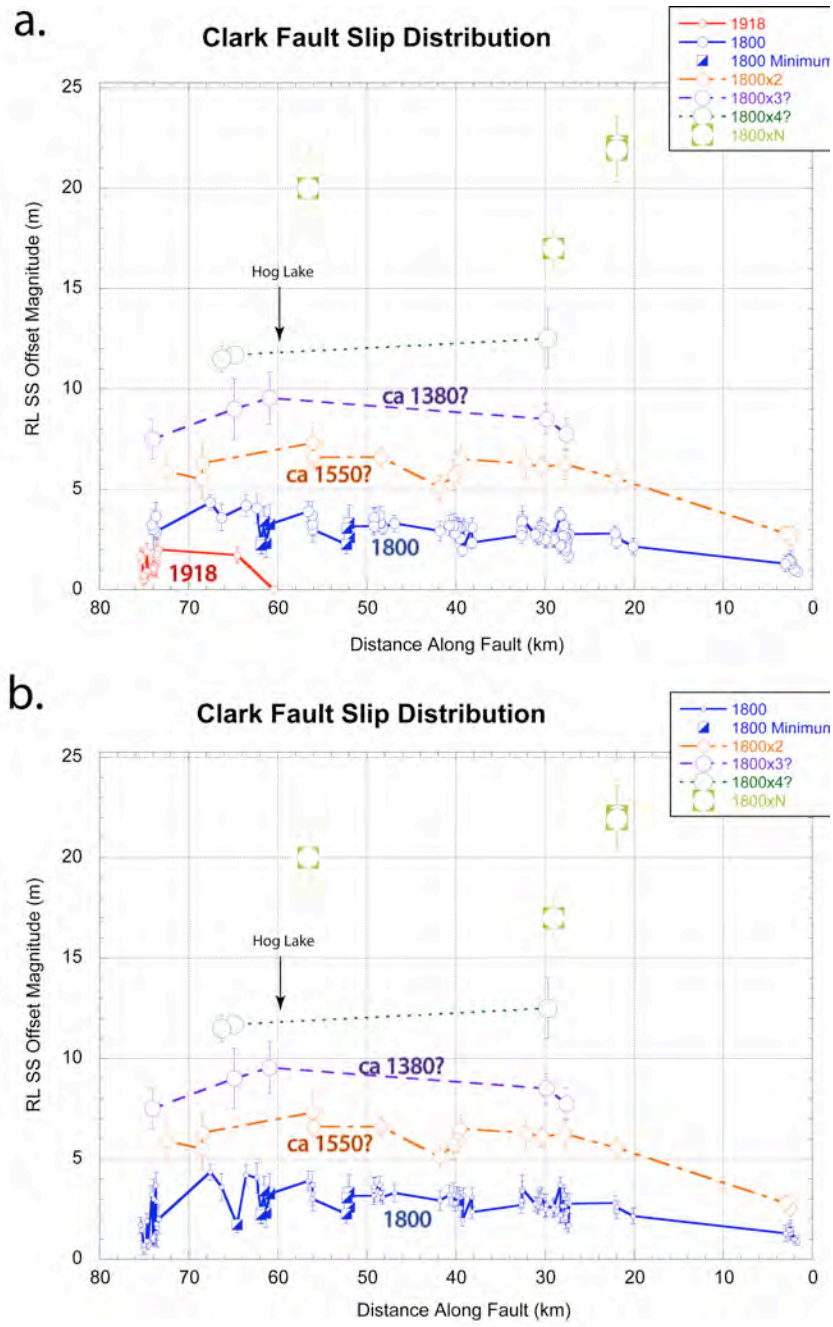


**Figure 5.** *Slip distribution models for geomorphic offsets collected along the Clark strand of the San Jacinto fault from highway S22 northwest to Blackburn Canyon, southeast of Hemet.*

In Summary, we have completed mapping of small geomorphic offsets for 75 km of the Clark fault from the southern end of Clark Valley (east of Borrego Springs) northwest to the mouth of Blackburn Canyon near Hemet. To the northwest, the flat valley bottom and young aggradation makes additional measurements with LiDAR impossible. Nevertheless, these data argue that much or all of the Clark fault, and possibly also the Casa Loma fault, fails from end to end in large earthquakes. We also recognize the likely rupture from the 1918 earthquake, which broke a short ~15 km section of the fault in Blackburn Canyon, apparently due to lower displacement in that area in the ca 1800 event.

**References**


Ellsworth, W. L., 2010, The San Andreas fault system, California: U.S. Geological Survey Professional Paper 1515, p. 24

Evans, J. S., Hudak, A. T., 2007, A multiscale curvature algorithm for classifying discrete return LiDAR in forested environments: IEEE Transactions on Geoscience and Remote Sensing, v. 45, no. 4, p. 1029-1038.

Middleton, T.J., 2006, Tectonic geomorphology of the southern Clark fault from Anza southeast to the San Filipe Hills: Implications of slip distribution for recent past earthquakes. Unpublished MS thesis, San Diego State University, 95 p.

Rockwell, T. K., and Y. Ben-Zion, 2007, High localization of primary slip zones in large earthquakes from paleoseismic trenches: Observations and implications for earthquake physics, J. Geophys. Res., 112, B10304, doi:10.1029/2006JB004764.

Rockwell, T.K., Seitz, G., Dawson, T., Young, J., 2006, The long record of San Jacinto fault paleoearthquakes at Hog Lake: Implications for regional patterns of strain release in the southern San Andreas fault system: Seismological Research Letters, v. 77, no. 2, p. 270.

Rolfe, F., and Strong A.M., 1918, The earthquake of April 21, 1918, in the San Jacinto Mountains: Bulletin of the Seismological Society of America, v. 8, p. 63-67.

Sander, C.O., McNally, K., and Kanamori, H., The state of stress near the Anza Seismicity Gap, San Jacinto fault zone, southern California, in Geology of the San Jacinto Mountains, Field trip Guidebook, 9, (eds. A.R. Brown and R.W. Ruff), p.61-67.

Sanders, C.O., and Kanamori, H., 1984, A seismotectonic analysis of the Anza Seismic Gap, San Jacinto fault zone, Southern California: Journal of Geophysical Research, v. 89, no. B7, p. 5873-5890.

Sharp, R.V., 1967, San Jacinto fault zone in the Peninsular Ranges of Southern California: Geological Society of America Bulletin, v. 78, p. 705-730.

Toppozada, T.R., Real, C.B., and Parke, D.L., 1981, Preparation of isoseismal maps and summaries of reported effects for pre-1900 California earthquakes: Open File Report 81-11 SAC, California Division of Mines and Geology, Sacramento.